UNITED NATIONS EDUCATIONAL, SCIENTIFIC AND CULTURAL ORGANIZATION
INTERNATIONAL ATOMIC ENERGY AGENCY
INTERNATIONAL CENTRE FOR THEORETICAL PHYSICS
I.C.T.P., P.O. BOX 586, 34100 TRIESTE, ITALY, CABLE: CENTRATOM TRIESTE

SMR.959 - 23

***MINIWORKSHOP ON STRONG ELECTRON CORRELATIONS***
***"Disorder and Interaction in Quantum Systems and Their Classical Analogs"***

**(1 - 19 July 1996)**

---

# "Spin Waves Throughout the Brillouin Zone of a Double-Exchange Ferromagnet"

**Gabriel Aeppli**
**N.E.C. Research Institute**
**4 Independence Way**
**Princeton, NJ 08540**
**U.S.A.**

---

***These are preliminary lecture notes, intended only for distribution to participants.***

# Spin Waves Throughout the Brillouin Zone of a Double-Exchange Ferromagnet

T.G. Perring[(1)], G. Aeppli[(2)], S.M. Hayden[(3)], S.A. Carter[(4)], J.P. Remeika[(4)*], and S-W Cheong[(4)]

[(1)] *ISIS Facility, Rutherford Appleton Laboratory, Oxon, OX11 0QX, UK*

[(2)] *NEC, 4 Independence Way, Princeton, NJ 08540, USA*

[(3)] *H.H. Wills Physics Laboratory, University of Bristol, Bristol BS8 1TL, UK*

[(4)] *AT&T Bell Laboratories, Murray Hill NJ 07974, USA*

(February 19, 1996)

## Abstract

We use inelastic neutron scattering to measure the spin wave dispersion throughout the Brillouin zone of the double-exchange ferromagnet $La_{0.7}Pb_{0.3}MnO_3$. Magnons with energies as high as 95 meV are directly observed and an unexpectedly simple Heisenberg Hamiltonian, with solely a nearest-neighbour coupling of 8.79±0.21 meV accounts for the entire dispersion relation. The calculated Curie temperature for this local moment Hamiltonian overestimates the measured Curie point (355 K) by only 15%. Raising temperature yields unusual broadening of the high frequency spin waves, even within the ferromagnetic phase.

PACS numbers: 71.27.+a, 75.30.Ds, 75.50.Cc

---

* Deceased

The past few years have witnessed a great revival [1] in the study of doped rare earth perovskite manganites [2], $R_{1-x}X_xMnO_3$ (R=La,Pr,Nd, X=Ca,Ba,Sr,Pb), because of the colossal magnetoresistance effects that have been observed. A thousandfold decrease in resistivity in an applied field has been reported for thin films of $La_{0.67}Ca_{0.33}MnO_3$, for example, and there is strong interest in these materials is both because of potential technological applications and fundamental questions relating to metallic band formation. The parent compounds are insulating antiferromagnets [3], such as $La^{3+}Mn^{3+}O_3^{2-}$, into which carriers can be introduced by chemical substitution onto the lanthanide sites with $X^{2+}$. With sufficient doping, the compounds can become metallic ferromagnets which undergo transitions to paramagnetic states at Curie points $T_C$ comparable to room temperature. A large decrease in electrical conductivity, $\sigma$, which appears to be controlled solely by the field- and temperature-dependent magnetisation, $M$, accompanies these transitions [4,5]. Of largest recent interest is that near $T_C$ the magnetic susceptibility is high so that $\sigma$ as well as $M$ is very field-sensitive.

The experimental study of the transport, thermodynamics and magnetic order in the doped cubic perovskite manganites has a long and distinguished history [2,3], as does corresponding theoretical work [4-6]. The properties of $La^{3+}_{1-x}X^{2+}_x(Mn^{3+}_{1-x}Mn^{4+}_x)O^{2-}_3$ are usually explained by double-exchange theory [4]. Crystal fields split the Mn $3d$ orbitals into three localised $T_{2g}$ orbitals, and two higher energy $E_g$ orbitals which are strongly hybridised with the oxygen $p$ orbitals. Each Mn ion has a core spin of $S = 3/2$, and a fraction $(1-x)$ have an extra electron in the $E_g$ orbitals with spin parallel to the core spin due to strong intrasite exchange. The electron can hop to an adjacent Mn site with unoccupied $E_g$ orbitals, without loss of spin polarisation [4], but with an energy penalty arising from the intrasite exchange that varies as

the cosine of half the angle between the core spins. The model accounts qualitatively for ferromagnetic alignment of the spins and carrier mobility that depends on the relative orientation of the Mn moments, which near $T_C$ will therefore be strongly dependent on the applied magnetic field.

Surprisingly, to the best of our knowledge, there exist no measurements [7,8] of the magnetic dynamics throughout the Brillouin zone in any of the ordered magnetic states of these interesting materials. The spectrum of magnetic excitations is unique as a source of answers to questions as fundamental as whether a simple local moment model is appropriate for the magnetic dynamics, and more specifically, what the effective Hamiltonian and the corresponding coupling constants are. We have therefore used inelastic neutron scattering to measure the magnetic excitations between 10 meV and 100 meV in $La_{0.7}Pb_{0.3}MnO_3$, a metallic ferromagnet with $T_C$ = 355 K. At 10 K, there are clearly resolved spin waves up to the zone boundary along all major symmetry directions. A ferromagnetic Heisenberg Hamiltonian including only a nearest-neighbour coupling which yields an overall magnon bandwidth of 108 meV is sufficient to describe the data, as well as, to within 15%, the Curie temperature of the compound. This simplicity of the effective spin Hamiltonian for $La_{0.7}Pb_{0.3}MnO_3$ is surprising given that the parent compound, $LaMnO_3$, is an antiferromagnet and that there are strong interactions between carriers and magnetic moments as evidenced by the collapse of the electrical resistivity below $T_C$. On warming, however, the carriers clearly manifest themselves in the second discovery of our research, namely the heavy damping of very high-frequency ($\approx$100meV) spin waves even below $T_C$.

The sample used in our neutron scattering measurements is a 1.86 g single crystal of $La_{0.7}Pb_{0.3}MnO_3$ grown from a lead oxide flux following the method of [9]. Crystals such as this have a slight rhombohedral distortion at low temperatures. However, given the twinning of our crystal and the resolution of the neutron experiment, we take the sample to be cubic with lattice constant $a_0 = 3.9$Å [9], equal to the separation between neighbouring Mn ions. We have measured the temperature-dependent resistivity and low-field magnetisation, $M$, obtained for a small sample from the same growth batch. $M$ rises sharply below $T_C = 355$ K, and there is a concomitant drop in resistivity, as is typical for $LaMnO_3$ samples doped to achieve ferromagnetism. Using magnetic neutron diffraction [3] we have confirmed that the Curie temperature is also 355 K for the larger crystal employed for our inelastic experiments.

We performed the neutron scattering measurements using the HET (High Energy Transfer) spectrometer at the pulsed spallation source ISIS of the Rutherford-Appleton Laboratory. HET is a direct geometry time-of-flight spectrometer [10], with a Fermi chopper in front of the sample whose phase with respect to the pulse can be chosen to fix the incident beam energy at any desired value. The neutron flight times give the energies of the scattered neutrons, and hence the energy transfers, $\hbar\omega$. Together with the scattering angle and the sample orientation, they also yield the momentum transfers $\mathbf{Q}$. One method for examining the dispersion surfaces of the normal modes of single crystals with triple-axis spectrometers is to plot the experimental intensities as a function of momentum transfer along some symmetry direction for fixed energy transfer. Given a multi-detector chopper spectrometer with fixed incident energy $E_i$, it is possible to measure scans along symmetry directions without rotating the sample [10]. In general, the energy transfer will vary along these directions. Even so, with a judicious choice of $E_i$ and sample orientation, one can achieve scans along the chosen

directions for which the energy transfer is almost constant, as illustrated in Fig. 1(a). Near reciprocal lattice points this yields a pair of peaks corresponding to counter-propagating modes with wavenumbers specified by the intersection of the surfaces defined by the nearly constant $\hbar\omega$ scan and the dispersion relation. Fig. 1(b) shows data for a scan centred on $\hbar\omega$ = 18 meV obtained along the (1,1,0) direction for our sample of $La_{0.7}Pb_{0.3}MnO_3$ at 10 K. As for the analogous triple-axis scan, the slightly different shapes and intensities of the two peaks are due to resolution effects which are well-understood, as indicated by the excellent agreement between the data and the solid line representing the convolution of the instrumental response function and the theoretical cross-section for spin waves in a nearest-neighbour exchange coupled Heisenberg ferromagnet. To allow for possible damping processes, for example decay into electron-hole pairs, the spin wave cross-section has been convolved with a damped simple harmonic oscillator. This reduces to delta functions in the limit of light damping.

We have used a number of incident beam energies (50, 100, and 200 meV) and sample orientations to obtain data such as those in Fig. 1(b) for positions along all major symmetry directions. The locus of peaks found in a sufficiently large number of scans provides complete knowledge of the dispersion relation. Fig. 2 shows the outcome of our survey, which reveals a net magnon bandwidth of approximately 100meV. Fig. 3(a), which presents classic time-of-flight scans for two fixed detector angles, demonstrates that the high energy magnons (solid circles) near the (½,½,½) zone boundary point are well-defined at 10 K. This implies that well within the ferromagnetic and metallic phase, there is little damping of the spin waves via interactions with the carriers. As a technical aside, note that as in Fig. 1, the two peaks in Fig. 3 (solid circles) are derived from the intersection of the phase-space trajectory of the

neutrons with the spin wave dispersion surface near a high symmetry point. We are thus, again as in Fig. 1, seeing counter-propagating magnons on either side of such a point, in this case the (½,½,½) zone boundary point rather than the (0,1,0) zone centre. For the higher angle scattering (open circles), the momentum transfers are far away from (½,½,½), so that the data are representative of the non-magnetic scattering for $\hbar\omega$ › 45 meV. Near the edge of the scan below 45 meV, there is spin wave scattering which, using the model described below can be understood simultaneously with the high energy modes.

One of the major open questions in the field of the doped manganites concerns the appropriate effective spin Hamiltonian in the ordered state. A general candidate is the Heisenberg form with couplings $J_{ij}$ between pairs of spins at sites $\mathbf{R}_i$ and $\mathbf{R}_j$,

$$H = -\sum_{ij} J_{ij}\mathbf{S}_i \cdot \mathbf{S}_j \tag{1}$$

For a ferromagnetic ground state, the corresponding spin wave dispersion relation is

$$\hbar\omega(\mathbf{Q}) = \Delta + 2S(J(\mathbf{0}) - J(\mathbf{Q})) \tag{2}$$

where

$$J(\mathbf{Q}) = \sum_j J_{ij} e^{i\mathbf{Q}\cdot(\mathbf{R}_i - \mathbf{R}_j)} \tag{3}$$

In Eq. (2) and Eq. (3), we have specialised to the case of a Bravais lattice, which implies that $J(\mathbf{Q})$ will be independent of which site $\mathbf{R}_i$ is chosen as the origin. Also, we have followed common practice and included a constant offset $\Delta$ to account for small anisotropies. Eq. 2 reduces to the well known form $\hbar\omega(\mathbf{Q}) = \Delta + Dq^2$ in the $q \to 0$, long wavelength, limit for arbitrary $J_{ij}$. The stiffness $D$ is a weighted average over all the exchange constants,

$D = (S/3)\sum_j J_{ij}\left|\mathbf{R}_i - \mathbf{R}_j\right|^2$ for a material with cubic symmetry. Given that the parent compound, $LaMnO_3$, is antiferromagnetic, we expected that we would need to include at least several terms in the Fourier series, Eq. (3), to account for the ensuing complexity of the effective interactions in $La_{0.7}Pb_{0.3}MnO_3$. More specifically, we anticipated softness in the spin wave spectrum near zone boundary points such as (½,0,0), (½,½,0), and (½,½,½). Such softness is not observed. Indeed, a single ferromagnetic nearest neighbour coupling, $2J_1S = 8.79 \pm 0.21$ meV, yielding the dispersion relation,

$$\hbar\omega(\mathbf{Q}) = \Delta + 4J_1S\left(3 - \cos(q_x a_0) - \cos(q_y a_0) - \cos(q_z a_0)\right) \qquad (4)$$

is entirely sufficient to account for the data in Fig. 2. Our fits also yield a small value for the effective gap, $\Delta = 2.51 \pm 0.46$ meV, which is well below the low frequency cut-off of our measurements which have been restricted to incident neutron energies of 50 meV and above. Adding second and third nearest-neighbour exchange constants, $J_2$ and $J_3$, does not improve the fit. The values obtained are $2J_2S$ = -0.09±0.24 meV (second nearest neighbour only), and $2J_2S$ = -0.43±0.35 meV, $2J_3S$ = 0.44±0.36 meV (second and third nearest neighbour), with small changes in each case to the values of $J_1$ and $\Delta$ similar to the errors in these quantities.

We have established that the effective Hamiltonian for the spins in $La_{1-x}Pb_xMnO_3$ with x=0.3 is that for a simple cubic Heisenberg ferromagnet with a single nearest-neighbour coupling. For the same model Hamiltonian, the mean field value for the Curie temperature is $4J_1S(S+1)/k_B$ or, in terms of the magnon bandwidth, $E_{ZB}(S+1)/6k_B$, where $E_{ZB} \equiv 24J_1S \equiv \hbar\omega(\mathbf{Q} = (\frac{1}{2},\frac{1}{2},\frac{1}{2}))$. For $S$ we use the mean spin on the manganese ions, $S = 3/2 + (1-x)/2 = 1.85$, as suggested by the double-exchange theory [4-6] and which

correctly gives the measured magnetisation at $T = 0$ K [11]. Together with our measured value of $2J_1S$, we calculate a mean field $T_C^{MF} = 581$ K for our sample. It is well known that fluctuations reduce the Curie temperature from $T_C^{MF}$ even for three-dimensional local moment ferromagnets. In particular, for the simple cubic nearest-neighbour Heisenberg ferromagnet, fluctuations reduce $T_C$ to $(J_1/k_B)(2.90S(S+1)-0.36)$ [12]. When we evaluate this quantity, again with $S = 1.85$ and the measured value of $2J_1S$, the expected Curie temperature is 410 K, only 15% larger than the measured value of 355 K.

Both because of the consistency of the Curie temperature with the magnon bandwidth and because of the simplicity of the low temperature spin waves, $La_{0.7}Pb_{0.3}MnO_3$ appears to be a very conventional ferromagnet. More specifically, since an effective spin Hamiltonian containing only nearest-neighbour couplings describes our neutron data, theoretical procedures which average the carrier motion over many bonds seem to be correct for $La_{1.7}Pb_{0.3}MnO_3$. The validity of such averaging would also mean that the transport properties simply follow the magnetisation, as is actually suggested by zero-frequency (i.e. static) bulk experiments [5,6]. Inelastic neutron scattering affords an opportunity to test whether in the dynamics of the magnetism the conduction electrons play a less trivial role, especially as $T_C$ is approached. It turns out that raising temperature within the ferromagnetic phase has a dramatic effect on the high frequency magnons. Fig. 3(b) shows that these excitations broaden to the point of virtually disappearing on warming from 10 K to 290 K, over which range the ferromagnetic order has changed relatively little ( $M(T)/M(0) = 0.75$ at $T/T_C = 0.8$ [5]). Both the 10 K and 290 K spin waves were fitted to the convolution of the instrumental resolution and a damped simple harmonic oscillator, with eigenfrequencies determined by Eq. 2, with $J$

allowed to vary but with $\Delta$ constrained to zero. The fitted inverse lifetime $\gamma$ for the high frequency magnons increases from $10 \pm 2$ meV at 10 K to $27 \pm 5$ meV $\approx k_B T$ at 290 K. In contrast, the lower energy magnons shown in Fig. 1(b) remain well defined, with $\gamma$ increasing only to $5 \pm 1$ meV. In the classic insulating ferromagnet EuO, the magnons remain much better-defined throughout the Brillouin zone even at similar reduced $T/T_C$ [13]. For example, at the (½,½,½) point of this (face centred) cubic material and $T/T_C = 0.86$, the measured inverse spin wave lifetime is $0.1\, k_B T$. It therefore appears that the same scattering mechanisms responsible for the many unusual bulk attributes of the manganites are at work to heavily damp the high frequency magnons even below $T_C$ in $La_{0.7}Pb_{0.3}MnO_3$. That higher frequency properties are still evolving below $T_C$ even when low frequency quantities are already tending towards saturation is also clear in the frequency-dependent optical conductivity recently reported for $La_{1-x}Sr_xMnO_3$ [14].

We have carried out the first measurement of the spin waves outside the small-$q$ regime for a metallic perovskite manganite. The outcome is that at low temperatures, there are well-defined spin waves throughout the Brillouin zone. The dispersion relation is that for a simple cubic ferromagnet with one significant free parameter, an effective nearest-neighbour Heisenberg coupling, which also accounts for the Curie temperature of the material to within 15%. This represents an unexpected and extraordinary simplification of the spin physics in a material whose parent compound is an antiferromagnetic insulator. One could well have expected that the interactions responsible for the latter might become apparent at short wavelengths in the ferromagnet. Indeed, in the superconducting cuprates, the magnetic fluctuations possess a much more complex wavevector-dependence [15] with certain short-wavelength features [16]

inherited from the parent antiferromagnets. Furthermore, many insulating ferromagnets such as EuS and EuO, and classic itinerant ferromagnets [17] ranging from Ni to $Pd_3Fe$, have more complicated low temperature spin waves. That analogous complexity is not found at 10 K in our manganite means that the only role of the charge carriers, as far as the low $T$ and low $\omega$ properties are concerned, is to fix a single effective exchange constant. However, our measurements are the first to show that at high T and high $\omega$ they acquire a more interesting role, that of heavily damping the spin waves near the zone boundary.

We are grateful to P.B. Littlewood, A. Millis, H.A. Mook, A.P. Ramirez, Y. Tokura, and C.M. Varma for helpful discussions.

## References


[1] See e.g. R.M. Kusters *et al.*,Physica B **155** 362 (1989); R. von Helmolt *et al.*, Phys. Rev. Lett. **71**, 2331 (1993); K. Chahara *et al.*, Appl. Phys. Lett. **63**, 1990 (1993); S. Jin *et al.*, Science **264** 413 (1994); A Asamitsu *et al.*, Nature **373** 407 (1995)

[2] G.H. Jonker and J.H. van Santen, Physica **16**, 337 (1950); J.H. van Santen and G.H. Jonker, Physica **16**, 599 (1950)

[3] E.O. Wollan and W.C. Koehler, Phys. Rev. **100**, 545 (1955).

[4] C. Zener, Phys. Rev. **82**, 403 (1951); P.W. Anderson and H. Hasegawa, Phys. Rev. **100**, 675 (1955); P-G. de Gennes, Phys. Rev. **118**, 141 (1960)

[5] C.W. Searle and S.T. Wang, Can. J. Phys. **48**, 2023 (1970)

[6] Very recent theory is by N. Furukawa, J. Phys. Soc. Jpn. **63**, 3214 (1994), and comparison between experiment and this theory is given by Y. Tokura *et al.*, J. Phys. Soc. Jpn. **63**, 3931 (1994).

[7] The spin wave stiffness found in the present work has been reported by A. Millis *et al.*, Phys. Rev. Lett. **74**, 5144 (1995).

[8] After we carried out the research described in this paper, A. Millis made us aware of a preprint by M.C. Miller *et al,* who describe neutron measurements of spin waves in the long-wavelength limit for $La_{1.7}Sr_{0.3}MnO_3$.

[9] A.H. Morrish *et al.*, Can. J. Phys. **47**, 2691 (1969).

[10] C.G. Windsor, *Pulsed Neutron Scattering* (Taylor and Francis, London, 1981). Chopper spectrometers are in quite common use for investigations of dispersive magnetic excitations in single crystals. See *e.g.* T.G. Perring *et al.*, J. Appl. Phys. **69**, 6219 (1991); S.M. Hayden *et al.*, Phys. Rev. Lett. **67** 3622 (1991); D.A. Tennant *et al.*, Phys. Rev. Lett. **70**, 4003 (1993);

S. Itoh *et al.*, Phys. Rev. Lett. **74**, 2375 (1995); T.G. Perring *et al.*, Physica B **213&214**, 348, (1995).

[11] L.K. Leung *et al.*, Can. J. Phys. **47**, 2697 (1969).

[12] G.S. Rushbrooke *et al.*, in *Phase Transitions and Critical Phenomena*, edited by C. Domb and M.S. Green (Academic, New York, 1974), Eq. 5.4

[13] H.A. Mook, Phys. Rev. Lett. **46**, 508 (1981).

[14] Y. Okimoto *et al.*, Phys. Rev. Lett. **75**, 109 (1995).

[15] T.R. Thurston *et al.*, Phys. Rev. B **40**, 4585 (1989); S-W. Cheong *et al.*, Phys. Rev. Lett. **67**, 1791 (1991).

[16] T. Imai *et al.*, Phys. Rev. Lett. **70**, 1002 (1993); S.M. Hayden *et al.*, preprint (1995); K. Yamada *et al.*, preprint (1995).

[17] For reviews, see articles by H.A. Mook and P.A. Lindgård in *Spin Waves and Magnetic Excitations*, vol. 22.1, edited by A.S. Borovik-Romanov and S.K. Sinha (North Holland, Amsterdam,1988).

# Figure Captions

FIG 1. (Nearly) constant energy transfer scan along the (1,1,0) direction through the (0,1,0) Bragg point, for incident energy $E_i$ = 50 meV, and crystal orientated with (-1,1,0) parallel to the incident beam. (a) The dotted line shows energy transfer as a function of momentum transfer for the scan. The magnon dispersion surface is indicated by the continuous line. Peaks in the scattered intensity are expected where the scan intersects the dispersion surface. Frames (b) and (c) show the scattering cross-section for T = 10 K and 290 K respectively. The two frames are normalised by monitor counts to have the same intensity scale. The different intensities of corresponding peaks in the two frames arise from the Bose occupation factor. Data collection times were 8 hours at 170 μA proton current with uranium target (b) and tantalum target (c).

FIG. 2. Spin wave dispersion along all major symmetry directions. The points correspond to measurements at 10 K; the statistical errors are smaller than the sizes of the points except where error bars are shown. Solid lines represent the dispersion relation for a Heisenberg ferromagnet with nearest neighbour coupling selected to best describe the data (see text).

FIG. 3. Energy scans obtained for fixed $E_i$ = 200 meV by integrating over the scattering angle ranges $2\theta$ = 9.31°-10.56° (closed circles) and $2\theta$ = 15.56°-17.43° (open circles). The data are normalised by detector solid angle as determined by scattering from a vanadium standard. Frames (a) and (b) show the scattering cross-section obtained for T = 10 K and 290 K respectively. The two frames are normalised by monitor counts to have the same intensity

scale. The solid lines in each frame are the results of the fit to a damped simple harmonic oscillator with eigenfrequencies given by Eq. 2, as described in the text.

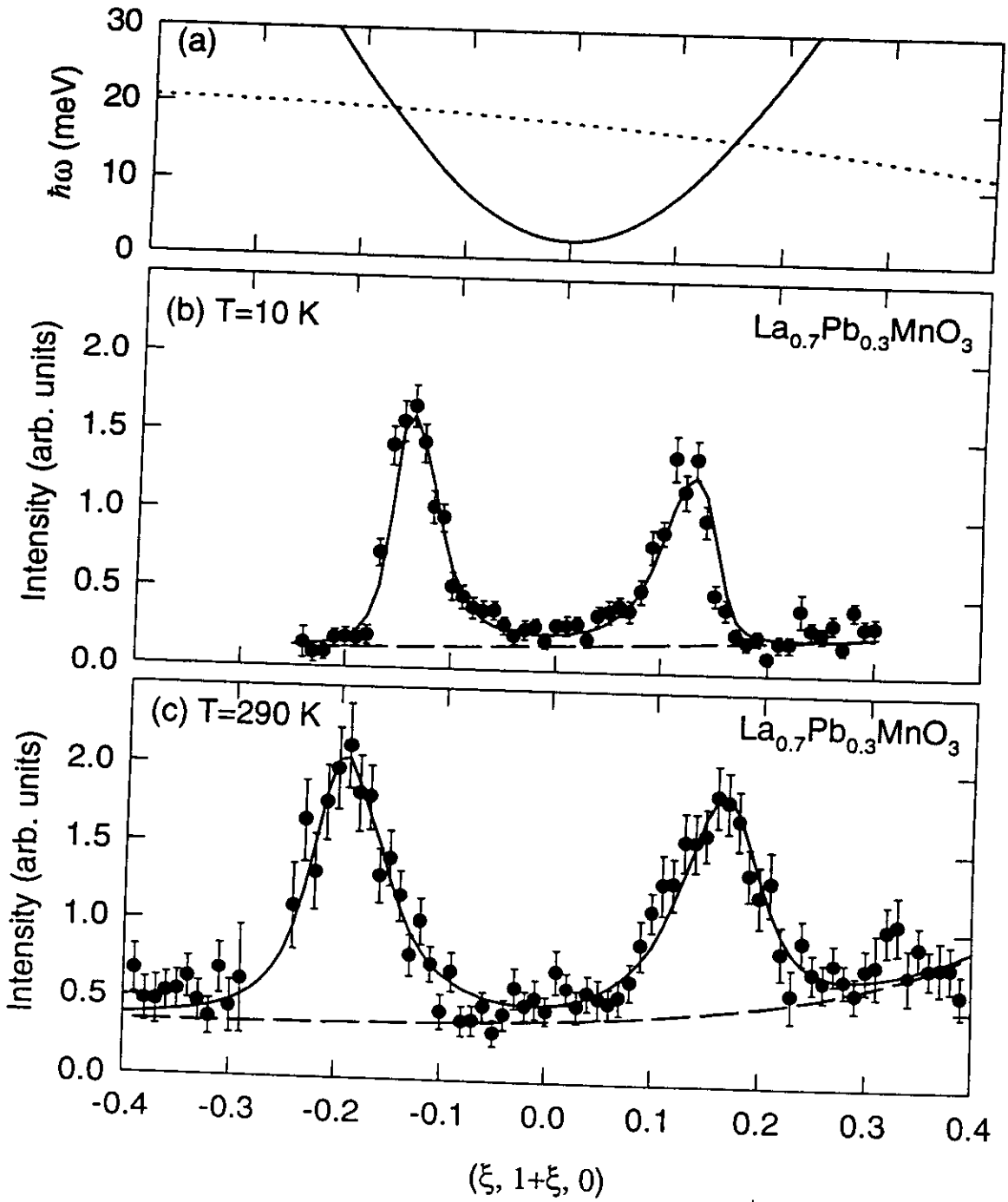


T. G. Perring et al  figure 1

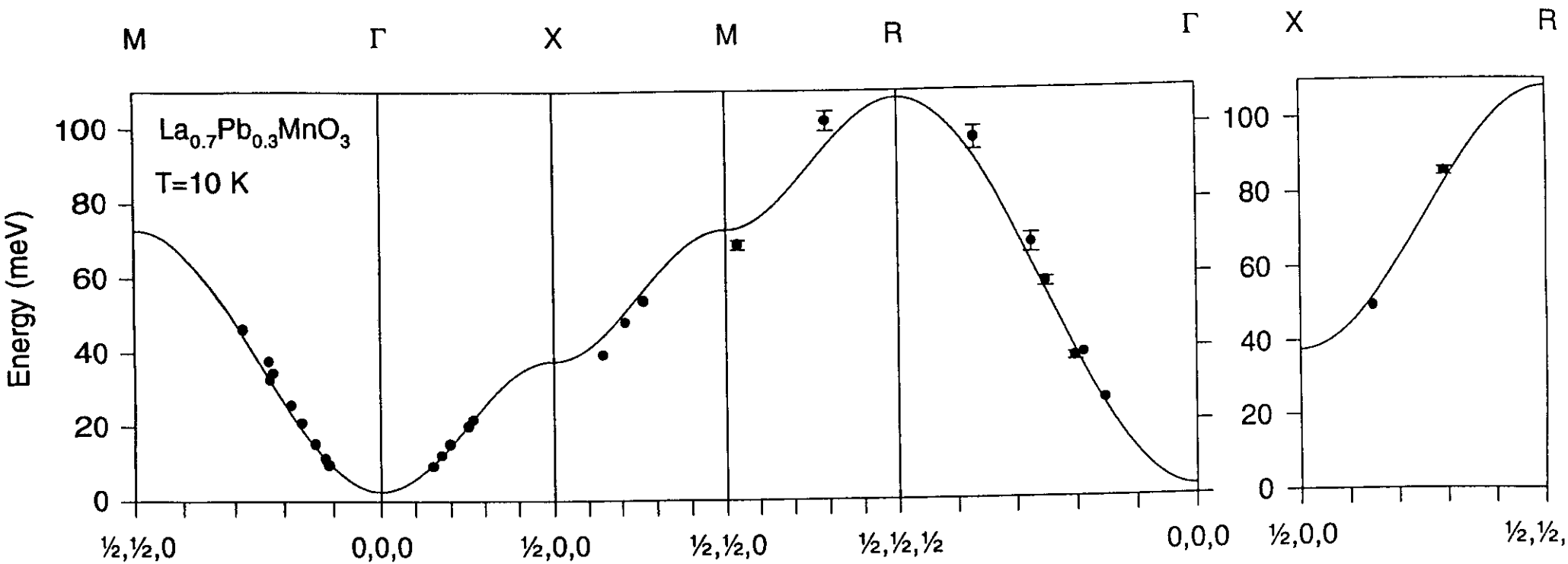


T. G. Perring et al  figure 2

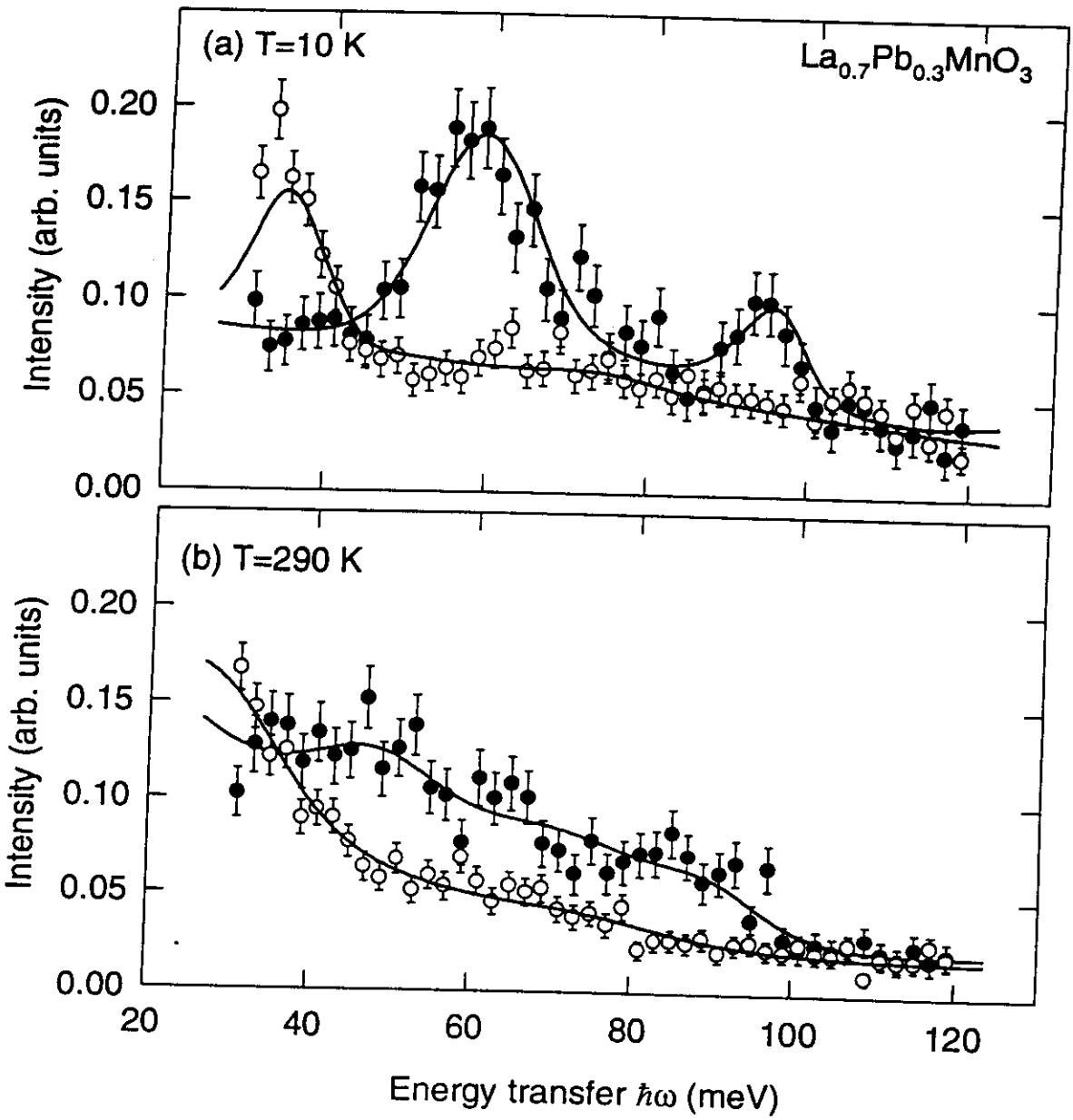


T.G. Perring et al

figure 3